ADVANCED MATERIALS
www.advmat.de

Soft Actuators Made of Discrete Grains

*Sophia Eristoff, Sang Yup Kim, Lina Sanchez-Botero, Trevor Buckner, Osman Doğan Yirmibeşoğlu, and Rebecca Kramer-Bottiglio**

Recent work has demonstrated the potential of actuators consisting of bulk elastomers with phase-changing inclusions for generating high forces and large volumetric expansions. Simultaneously, granular assemblies have been shown to enable tunable properties via different packings, dynamic moduli via jamming, and compatibility with various printing methods via suspension in carrier fluids. Herein, granular actuators are introduced, which represent a new class of soft actuators made of discrete grains. The soft grains consist of a hyperelastic shell and multiple solvent cores. Upon heating, the encapsulated solvent cores undergo liquid-to-gas phase change, inducing rapid and strong volumetric expansion of the hyperelastic shell up to 700%. The grains can be used independently for micro-actuation, or in granular agglomerates for meso- and macroscale actuation, demonstrating the scalability of the granular actuators. Furthermore, the active grains can be suspended in a carrier resin or solvent to enable printable soft actuators via established granular material processing techniques. By combining the advantages of phase-change soft actuation and granularity, this work presents the opportunity to realize soft actuators with tunable bulk properties, compatibility with self-assembly techniques, and on-demand reconfigurability.

1. Introduction

Soft robots have garnered interest due to their potential ability to change shape in response to changing tasks or environments,[1–5] be robust to impacts and falls,[6–8] conform to the human body without restriction on the natural mechanics of motion,[9–13] and grasp delicate and diverse objects.[14–17] Furthermore, soft robots embed safety at the material level, and are generally accepted as a path toward human-safe co-robotics.[18,19]

Fluidic actuators are the most common artificial muscle technology employed in the soft robotics literature,[2,20–22] however, fluidic actuators typically require actuator-source tethering, limiting the mobility of the robot.[19–21,23,24] Alternatively, stimuli-responsive materials, such as hydrogels[25] and shape-memory polymers,[26–28] have been proposed to realize untethered, microscale actuation. However, these material-based actuators are often slow or only expand or contract axially, preventing use in applications that require volumetric expansions. To address such limitations of existing actuating materials, actuators based on the liquid-to-gas phase change of solvent inclusions encapsulated in a hyperelastic matrix have been realized. Phase-change actuators are capable of inducing rapid volumetric expansion similar to fluidic actuators, without being tethered to an external fluid source.[29–32]

Accepting the advantages of phase-change actuators, we now turn our attention to granular media. Granular assemblies, consisting of discrete grains, can be tuned to accomplish a variety of different responses. For example, favorable self-assembly of granular media can be achieved via modulating interparticle interactions and external stimuli,[33–36] and granular assemblies with different packing configurations have been shown to yield different bulk properties.[36–39] Furthermore, granular media can exhibit optimized changes in stiffness during jamming transitions, enabling tunable moduli.[16,40–44] When unjammed, the bulk material is compliant, and when jammed, the bulk material can achieve the stiffness of the grains. Finally, when mixed into carrier fluids, granular media can impart thixotropic behavior on the carrier fluid due to dynamic jamming,[45–48] enabling 3D printing of previously unprintable materials. With all the advantageous properties granular media has to offer, the technology has seen application in soft robotics,[49–52] medical devices,[53–55] flexible airfoils,[56] and programmable aggregate architecture.[57]

Here, we bring together the unique advantages of phase-change soft actuators and granular media to introduce soft granular actuators made of discrete, volumetrically expanding grains. A single active grain consists of multiple solvent cores encapsulated in a hyperelastic silicone shell (Ecoflex 00-30). At elevated temperatures, the encapsulated solvent vaporizes and increases the internal pressure of the hyperelastic shell, inducing volumetric expansion of the grain. The grains are independently capable of rapid, high-force microscopic actuation, and are also easily arranged into granular assemblies to form larger-scale bulk actuators. Furthermore, agglomerates of active grains can self-assemble from disordered arrangements to conform around objects and exhibit variable moduli. Finally, the use of grains suspended in a carrier solvent or resin enables compatibility with granular self-assembly and 3D printing techniques, offering the potential to print volumetrically expanding actuators into freeform patterns across scales.

S. Eristoff, S. Y. Kim, L. Sanchez-Botero, T. Buckner, O. D. Yirmibeşoğlu, R. Kramer-Bottiglio
School of Engineering and Applied Science
Yale University
9 Hillhouse Ave., New Haven, CT 06511, USA
E-mail: rebecca.kramer@yale.edu
S. Y. Kim
Department of Mechanical Engineering
Sogang University
35 Baekbeom-ro, Seoul 04107, Republic of Korea
The ORCID identification number(s) for the author(s) of this article can be found under https://doi.org/10.1002/adma.202109617.

DOI: 10.1002/adma.202109617

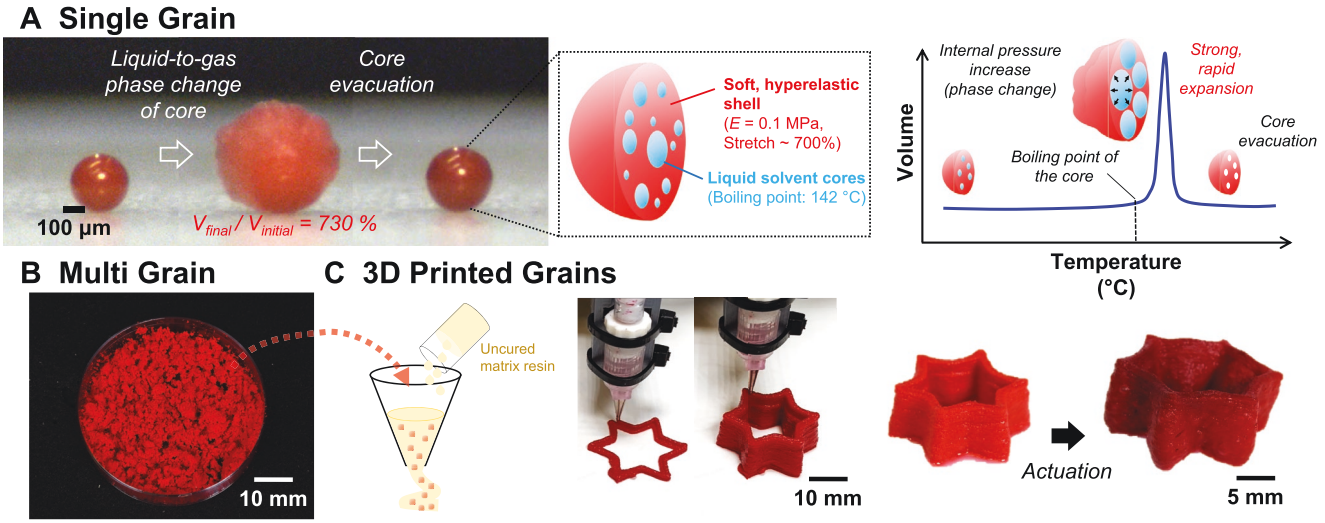

Figure 1. Overview of the volumetrically expanding grains. A) Working mechanism of a grain. When placed on a hot plate of 200 °C, the grain exploits the liquid-to-gas change of the encapsulated solvent cores, leading to a rapid volumetric expansion up to 730%. B) A group of grains, showcasing the scale of the high-throughput synthesis process. C) A mixture of the grains and uncured matrix resin enables 3D printing of freeform actuators.

2. Results

Figure 1 shows an overview of granular actuators and their scalable design space. A grain consists of a soft hyperelastic shell with multiple embedded solvent cores (Figure 1A). At elevated temperatures, a grain will volumetrically expand due to the liquid-to-gas phase change of the solvent cores. Post actuation, the grain's shell elastically recovers as the solvent cores evacuate. The active grains are prepared via a high-throughput double emulsion process, yielding large numbers of grains (Figure 1B). Incorporating the grains into uncured silicone resin enables printability, opening up the design space for freeform actuators (Figure 1C).

We first characterized the multicore hyperelastic grains and their manufacturing parameters (**Figure 2**). To synthesize grains, perfluorodecalin (PFD) is first emulsified in uncured silicone (Ecoflex 00-30). Thereafter, the resulting PFD/silicone mixture is poured into an aqueous medium of sodium alginate, where the mixture is then emulsified a second time (Figure S1, Supporting Information). Once the uncured silicone is broken down sufficiently, the shear-thinning thixotropic properties of the aqueous sodium alginate enables static-state solidification.[58] This double emulsion results in silicone grains with multiple solvent cores suspended in the aqueous continuous phase, which can be rinsed away after the silicone cures.

Optical microscopy images under transmittance light reveals the spherical shape of the grains (Figure 2A). The size of the grains is tunable by either modulating the viscosity of the sodium alginate medium or the shear rate during the second emulsification process (Figure S2, Supporting Information). In general, the higher the viscosity of the medium or the shear rate, the lower the mean diameter of the resulting grains, which is in agreement with existing emulsion processes.[58–60] When prepared at 500 rpm in a 3 wt% sodium alginate aqueous medium, the size distribution of the grains exhibits a normal distribution with a mean diameter of 162 µm (Figure 2B). Thermogravimetric analysis (TGA) reveals that each grain contains around 8 wt% PFD solvent when compared against neat silicone control spheres (Figure 2C), and cross-sectional scanning electron microscopy (SEM) images confirmed internal grain pockets where PFD was contained (Figure 2D). The neat control spheres absorbed <1 wt% of PFD when soaked in a PFD bath for 24 h, underscoring the need to encapsulate solvent within the grains.

To quantify actuation performance, we conducted actuation force measurements on a single grain using a dynamic mechanical analyzer (DMA) (Figure 2E). Elevating the temperature above the vaporization point of PFD (142 °C), the active grain produced a rapid actuation force of 62 kPa. In comparison, both neat control spheres and control spheres were soaked in PFD generated marginal forces <2 kPa, which is presumably due to the thermal expansion of the Ecoflex 00-30 matrix. The rapid expansion of a grain is attributed to the snap-through of its hyperelastic spherical shell as,

$$P = C\left(\frac{1}{\lambda} - \frac{1}{\lambda^7}\right) \tag{1}$$

where P and λ are the internal pressure and the stretch ratio of the grain respectively, and C is the material constant derived from various elastic properties (Equation (1), and Figures S3 and S4 and Section S1, Supporting Information).[61,62] Notably, the structural instability of the hyperelastic spherical shell gives rise to the near-instantaneous expansion of the grain via snap-through behavior, an actuation strong and fast enough to elicit jumping (Figure 2F and Movie S1, Supporting Information). The expanded grain obtained a rough surface texture as the individual pockets of solvent expanded, distinguished from the smooth wall of pristine grains, and underwent shape recovery as the encapsulated solvent evacuated (Figure 2G). The grains exhibited a volume increase of ≈125% due to plastic deformation at higher temperatures, which agrees with prior works.[63] Post-actuation, the grains are unable to undergo subsequent actuation sequences due to silicone permeability at high strains, thus leading to evacuation of the solvent cores.

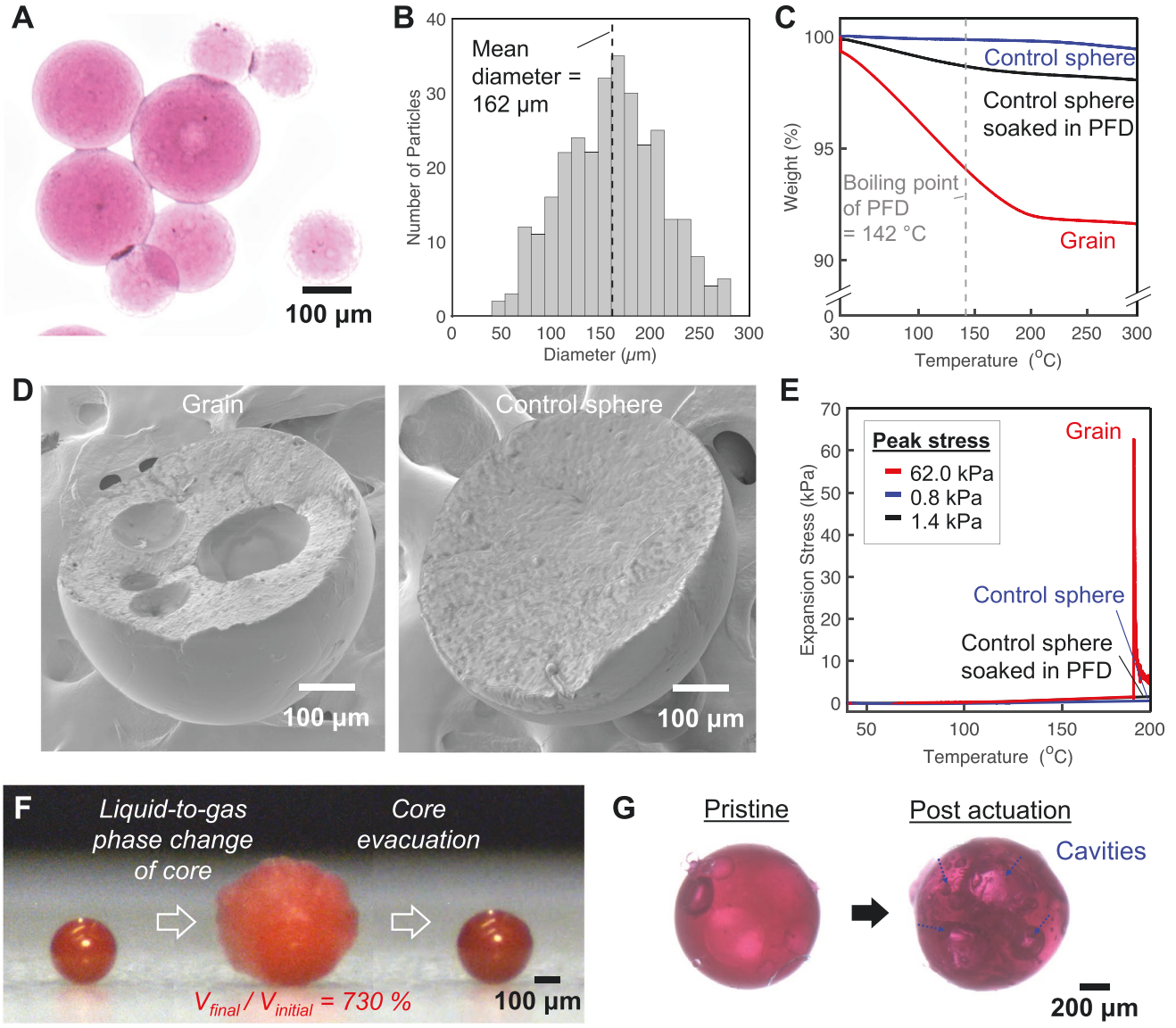

Figure 2. Characterization of the volumetrically expanding grains. A) Optical microscopy image of the multicore hyperelastic grains. B) Size distribution of the grains, controlled by a shearing speed during emulsification and viscosity of the sodium alginate medium (see Figure S2, Supporting Information). C) TGA results of the grains and control spheres prepared using identical materials and processes but without PFD inclusions. Control spheres are also soaked in a PFD bath but uptake a marginal amount of PFD. D) Cross-sectional SEM images of a grain and a control sphere. Multiple cavities in the grain serve to contain PFD solvent. E) Actuation force results of a grain and a neat control sphere with and without being soaked in PFD solvent. The grain exhibits rapid volumetric expansion past the boiling point of PFD, in stark contrast to control spheres. F) Time-lapse images of a jumping grain taken at 500 frames per second. G) Optical microscopy images of a grain prior to and post actuation. Multiple cores and cavities are visible.

The scalability of granular actuators—actuators made up of multiple or many volumetrically expanding grains—was investigated by embedding active grains into a silicone elastomer to realize a composite material (**Figure 3**). Since a concentration of the grains can be directly mixed into uncured silicone resin, the composite manufacturing process is easy to scale up and readily tailorable to control the bulk actuator properties (Figure 3A). Upon heating, the composite exhibits a rapid sequence of multiple actuation events as each embedded grain expands individually (Figure 3B and Movie S1, Supporting Information). Expansion stress measurement results reveal that the actuation force of a composite actuator with a grain fraction of 60 wt% is 150 times greater than that of the control specimens embedded with neat control spheres (Figure 3C). It is possible to modify the stress and strain properties of the composite by modulating the grain fraction, W_c (Figure 3D). Additionally, adjusting the grain fraction gives rise to different measured volumetric expansions, where higher grain fractions induce larger volumetric expansions (Figure 3E).

The active grains can be incorporated into a low-viscosity solvent like ethanol or water to enable drop-on-demand printing, as shown in previous works,[64–66] or even arranged without any liquid external media (in air). However, here we focus on incorporating grains into an elastic medium to showcase the

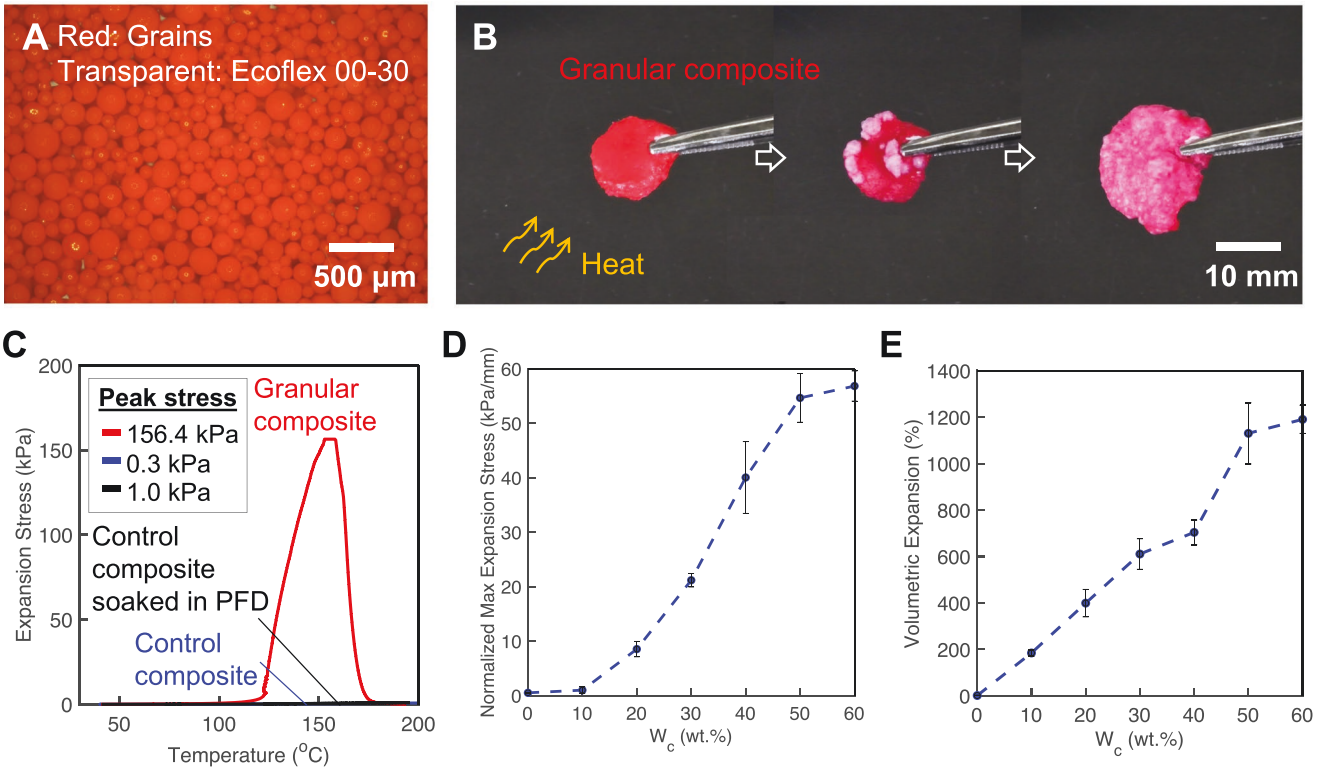

Figure 3. Characterization of the soft granular composite. A) Optical microscopy image of the composite actuator with embedded grains. B) Expansion of the granular composite when exposed to forced hot air. C) Actuation force results for the granular composite and control composites that replace the grains with neat control spheres (no PFD cores). The control composite with embedded control spheres shows negligible actuation. D) Actuation force results for the granular composite with varying grain concentrations, W_c. Increasing the W_c leads to an increase in actuation forces. E) Volumetric expansion results of the granular composite with varying grain concentrations, W_c. Increasing W_c leads to an increase in volumetric expansion, up to 1200%.

scalability and extrusion-based 3D printability of the grains (**Figure 4**). Our composite actuator with embedded active grains unlocks printable soft actuation, which has remained elusive in existing phase-change actuators. Typically, phase-change actuators exhibit low uncured viscosity due to the incorporated liquid solvent, rendering it impossible to achieve 3D printing of the material without the addition of viscosity enhancers.[29–31] However, in our method, the grains provide not only the solvent inclusions but also the viscosity enhancement of an otherwise unprintable low viscosity carrier resin, increasing the thixotropic response with increasing grain fraction (Figure 4A). The amplitude sweep in Figure 4B shows the linear viscoelastic region and the yielding region for our high fraction uncured granular composites (60 wt%) with a storage modulus (G') of 2830 Pa and a dynamic yield stress (σ_y) of 123 Pa. The ink can flow after the yield point but rapidly regains its structure after extrusion (Section S2, Supporting Information). The shape retention $\kappa = h/w$, where h and w are height and width of the printed filament respectively, remains >0.9 at a grain fraction $W_c =$ 60 wt% (Figure 4C), which is sufficient for 3D printing (Figure 4D and Movie S1, Supporting Information), thus enabling the freeform fabrication of soft actuators with highly varied designs.

We present the practical utility of both the granularity and actuation properties of the grains in **Figure 5**. The microscopic actuation of a single grain can be used to lift a mass 2000 times its own weight in less than 2 ms (Figure 5A and Movie S1, Supporting Information). When individual actuating grains are patterned onto a microscale soft cylinder and placed on a heat source, the grains in contact with the heat source sequentially expand to induce rolling locomotion (Figure 5B and Movie S1, Supporting Information). Furthermore, a collection of grains can be integrated into a soft pouch to give rise to a jamming gripper (Figure 5C and Figure S5 and Movie S1, Supporting Information).[16] The enclosed grains exhibit compliance at atmospheric pressure and when under vacuum pressure, the grains undergo jamming behavior, increasing the stiffness of the system and enabling gripping of the object. Because the grains can be utilized both as discrete components and in composite form, they serve as effective soft actuators across a variety of scales and applications (Figure 5D and Figures S6–S9 and Section S3, Supporting Information).

To demonstrate the potential for our granular composite actuator to be printed onto arbitrary structures, Figure 5E shows short segments of the granular composite printed directly onto a soft cylinder, enabling local curvatures along the inert filament. The working principle of the actuating filament can be extended to control the morphing of a 2D soft silicone film (Figure 5F and Movie S1, Supporting Information). Finally, the granular composite can be printed directly onto inanimate fabrics[67] to, for example, provide pronounced motion for gait or gripping behavior (Figure 5G and Movie S1, Supporting Information). Exploiting the scalability, dynamic tunability, and flow properties of granular media, coupled with the rapid

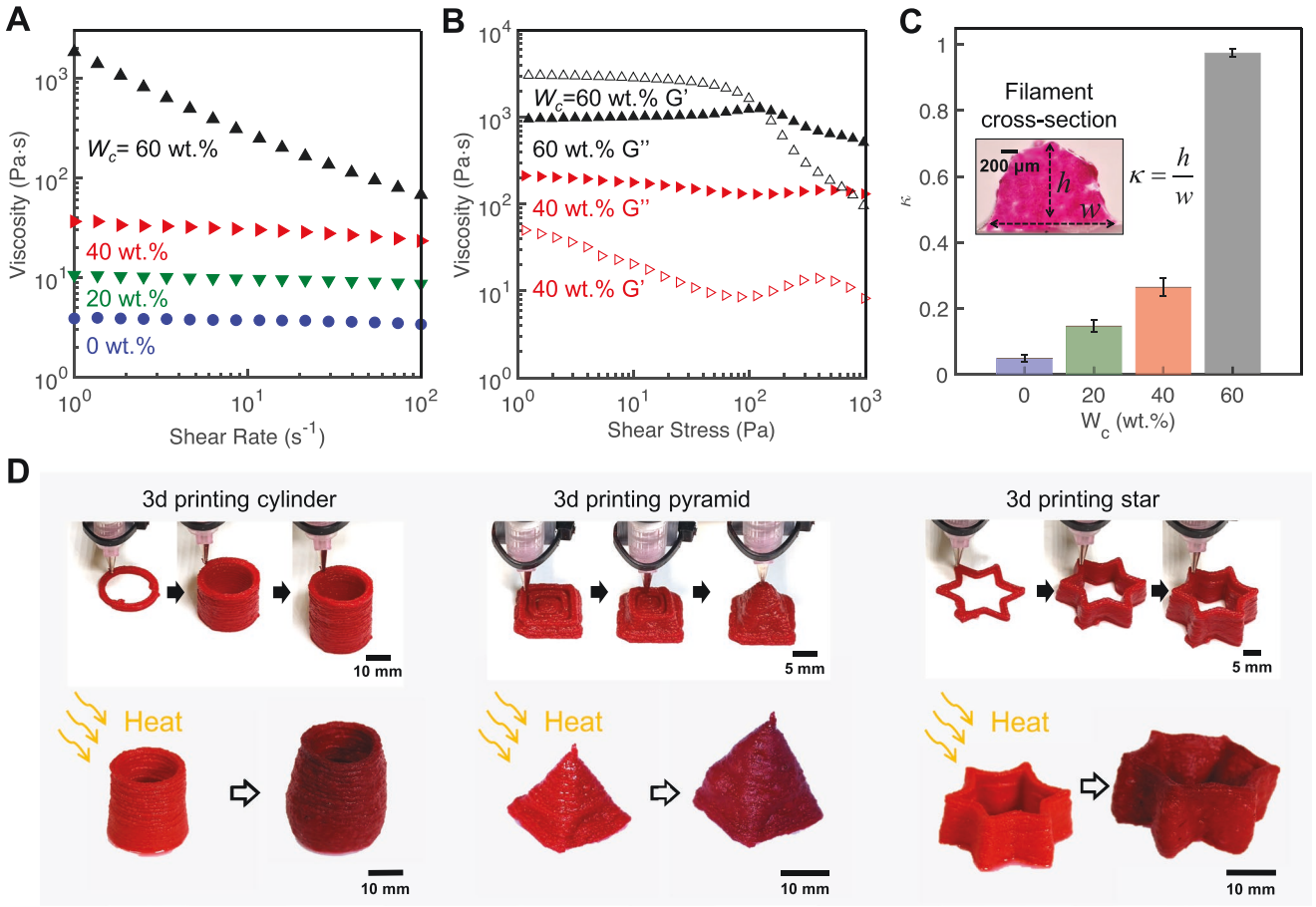

Figure 4. Printability of grains in a soft granular composite. A) Rheological behavior of Ecoflex 00-30 resin and grain mixtures. Shear thinning behavior of the mixture becomes apparent as the grain concentration, W_c, increases. B) Effect of the applied shear stress on the resin and grain mixture viscosity. Higher W_c enables printability. C) Shape retention of the mixture after printing on a flat surface as a function of W_c. D) 3D printing and actuation of soft granular actuators in a variety of shapes.

and strong volumetric expansions of phase-change actuators, actuating grains offer the potential to collectively broaden the design space of robotic systems.

3. Conclusion

We have developed granular actuators that exploit the advantageous properties of both granular media and phase-change actuators. Consisting of a hyperelastic shell and multiple PFD solvent inclusions, a single volumetrically expanding grain produces micro-actuation via thermally driven phase change of the solvent. The expanding grains can be used independently for micro-actuation, or in collectives for larger-scale actuation. Additionally, collections of grains exhibit variable bulk mechanical properties based on their configuration, assembly, and boundary conditions (e.g., jamming). When suspended in a carrier solvent or resin, the grains favorably modify the rheological properties in a way that enables stable 3D printing of bulk soft actuators. Via printing, inanimate objects can be easily augmented with widely varied soft actuator designs, displaying the multifaceted potential of the soft granular actuator.

Naturally, there are areas for improvement with this technology. By modulating particle size and interparticle interactions, we hypothesize control over particle self-assembly behavior, collectively enhancing granular actuator properties and manufacturing techniques by enabling optimized packing configurations and the opportunity to employ drop-on-demand techniques. We also expect to move beyond single-stroke actuation sequences to repeatable actuation of the grains by optimizing the constituent materials to prevent solvent evacuation. Additionally, we see a need for precise, localized command of actuator grains. Utilizing a range of solvents with distinct vaporization temperatures could enable controlled actuation sequences, while an addressable heating interface could allow us to specifically actuate certain grains within a cluster.

We see various potential applications for granular actuators in future works. Actuating grains can be switched from a solid-like to liquid-like state via confinement pressure, allowing the actuator to be rearranged into a variety of configurations on-demand, which implies a potential for rapid prototyping and high customization of soft actuators. We envision adaptable soft robots, with granular actuators that can flow within the body to sites where forces are needed.

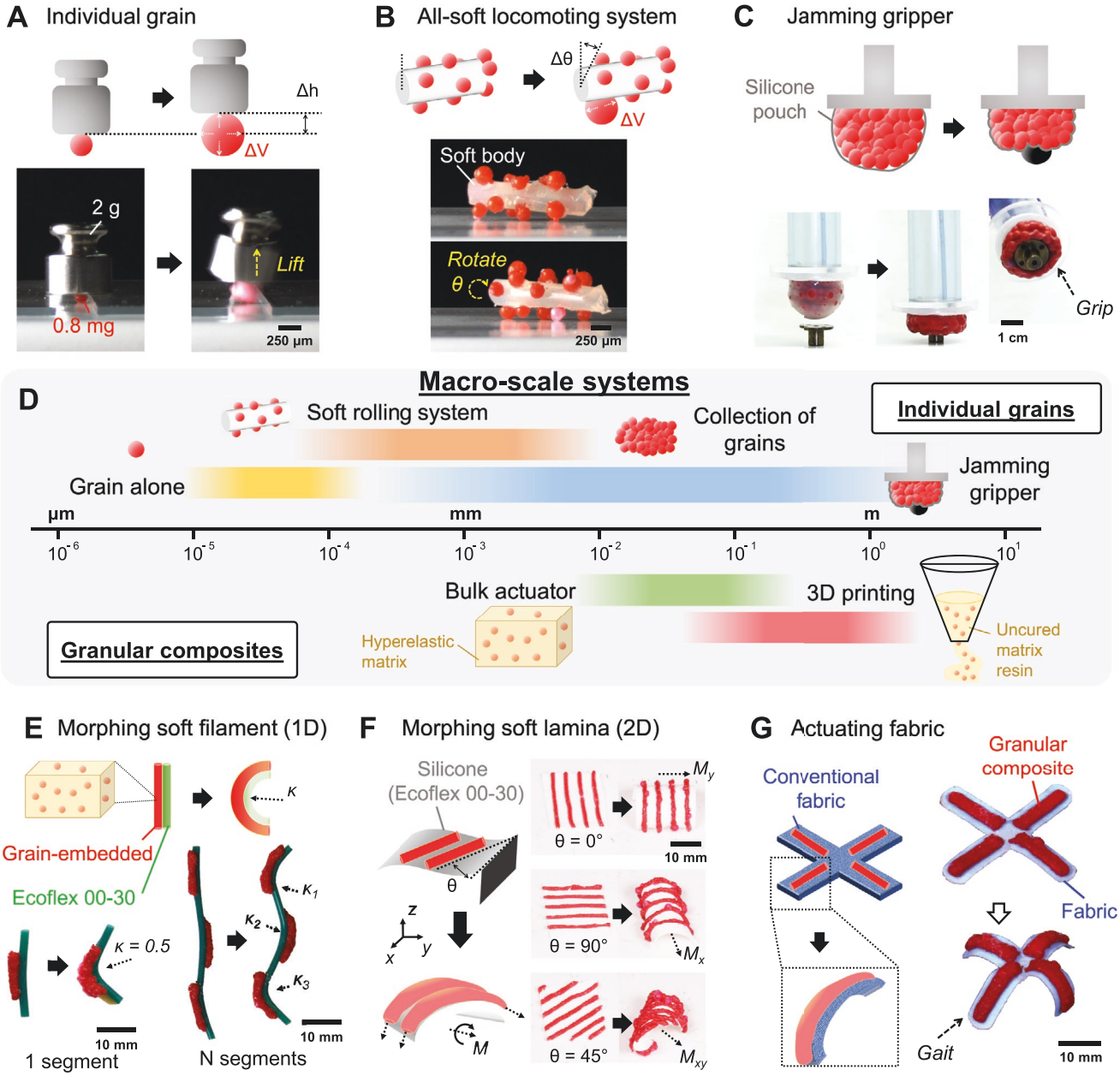

Figure 5. Multiscale design space of the grains in various applications. A) Actuation of a single grain allows lifting an object >2000 times heavier in less than 2 ms. B) Adhering grains onto a soft body realizes an all-soft locomoting system that can rotate due to the expansion of each grain. C) Under vacuum pressure, a collection of grains in a silicone pouch may undergo jamming behavior, enabling gripping of objects. D) Application space of the grains. Individual grains and granular composites act as effective actuators across scales. E) Printing the granular composite onto 1D inert soft filaments provides substantial morphing depending on patterning. F) Granular composite can be printed onto a 2D silicone laminae to direct its actuated curvature. G) Conventional fabrics can be granted motion when the granular composite is printed in a pattern.

Additionally, due to the printability of the granular composite, we foresee intricate, 3D actuators patterned alongside other components to achieve new levels of robotic material integration. Finally, we envision a generalized, easy-to-use, volumetrically expanding actuator that can replace the need for tethered air supplies. Given the vastly versatile potential of granular actuators, we are optimistic that this new class of actuation will open up broader design spaces for diverse robotic systems across scales.

4. Experimental Section

Materials: Platinum-cure silicone polymer Ecoflex 00-30, Platinum silicone cure accelerator Plat-Cat, Silc Pig silicone dye, silicone thinner, and SIL-Poxy adhesive were purchased from Smooth-On (Macungie, PA). Sodium alginate was purchased from Modernist Pantry (Eliot, ME, USA) and PFD (95% purity, vapor pressure of 0.88 kPa at 25 °C) was purchased from Sigma Aldrich (St. Louis, MO, USA).

Preparation of Grains: The sodium alginate solution was prepared by mixing a designated mass of sodium alginate into a volume of distilled

water. Higher concentrations of sodium alginate in water resulted in higher viscosity of the medium; a concentration of 3 wt% was used in this work (Figure S10, Supporting Information). This sodium alginate solution was mixed using an overhead mixer (IKA Eurostar 20) until completely homogeneous. Grains were created by mixing Ecoflex 00-30, cure accelerator, silicone thinner, red silicone dye (for better visualization), and PFD in a planetary mixer (ARE-310 Thinky) for 1 min at 2000 rpm. Subsequently, the polymer mixture was poured into the sodium alginate solution and mixed in the ARE-310 Thinky for another 10 min, at a designated speed (nominally 500 rpm). The mixture was placed in an oven at 80 °C for 1 h to cure. Finally, the mixture was filtered through an ASTM E-11 standard sieve and thoroughly rinsed with distilled water. Grains were stored in a suspension of PFD to prevent ambient evaporation of solvent prior to intended use.

Experimental: TGA was performed using a TGA Q50 from TA Instruments over a temperature range of 30–300 °C, at a rate of 10 °C min^{-1} in N_2 atmosphere. A grain size of ≈1 mm diameter was used for TGA analysis.

Actuation force measurements were performed using a DMA from TA Instruments (model 850) with a parallel compression plate fixture of 23 mm in diameter. Specimens were placed into a shallow aluminum dish machined such that the upper compression plate of the DMA fit neatly within its inner diameter. Each test began by equilibrating the chamber temperature to 40 °C. Next, contact with the specimen was ensured as an initial preload of 500 Pa was applied relative to the cross-sectional area of the specimen, and was allowed to stabilize for 2 min to mitigate the effects of any strain relaxation. After this point, the parallel plates remained stationary in an isostrain configuration. The temperature of the DMA chamber was then increased to 200 °C at a rate of 10 °C min^{-1} in a nominal air atmosphere. As the specimens activated, the blocked expansion force was measured. A grain size of ≈1 mm diameter was used for actuation force analysis of single grains. A grain size of ≈200 µm diameter was used for actuation force analysis of composite actuators. Since increasing the dimensions of the composite actuator sample, namely the thickness, could enable higher measured expansion stresses, the specimens must be normalized with regard to sample thickness (Figure S11, Supporting Information).

SEM images were obtained using a Hitachi SU-70 at 2 kV.

Rheological behavior of the uncured composite actuator was analyzed using an Anton Paar MCR 302 rheometer in a parallel plate geometry with a diameter of 25 mm and gap size of 1.5 mm. Shear rate was varied from 1 to 100 Hz with clockwise rotational motion at room condition. Dynamic oscillatory tests were performed with increasing amplitude stress up to 1000 Pa at a frequency of 1 Hz. A grain size of ≈200 µm diameter was used for rheological analysis of composite actuators.

High speed videos were captured at 500 frames per second using a Micro LAB110 from Vision Research.

3D Printing of Grains: A customized 3D printer attached with a Teflon-coated 18G (inner diameter: 1.041 mm) nozzle was used for additive manufacturing. A mixture of 60 wt% grains in uncured Ecoflex 00-30 was loaded into a 50 mL syringe and extruded using a high precision fluid dispenser. A grain size of ≈200 µm diameter was used. The pot life of the premixed material in the syringe was limited to a time of up to 45 min. However, this limited print time could be resolved by using an active mixing system commonly seen in literature.[68–70] Completed prints were then left to cure at room temperature for 4 h prior to actuation. The experimental setup with the modified printer is shown in Figure S12, Supporting Information, and the print parameters are displayed in Table S1, Supporting Information. Flow rate calculations and the printing process are discussed in Section S4, Supporting Information. Printed primitive shapes and their dimensions are shown in Figure S13, Supporting Information.

Demonstrations: The all-soft microscopic rolling system was prepared by adhering a group of grains onto a soft cylinder made of Ecoflex 00-30 by using SIL-Poxy adhesive. The jamming gripper was prepared by embedding grains of ≈3–5 mm in diameter into an Ecoflex 00-30 pouch. A standard vacuum pump was used for demonstrative purposes. For the composite actuator, a mixture of uncured Ecoflex 00-30 and grains were prepared at 60 wt% of grain concentration (W_c). A grain size of ≈200 µm diameter was used. The actuation of both the grains and composite actuator was achieved by placing them onto a hot plate set to a temperature of 200 °C or applying forced hot air. The authors noted that in the robotic fabric demonstration some slight discoloration of the fabric was visible due to heating, and that heat-resistant fabrics might mitigate this issue.

Supporting Information

Supporting Information is available from the Wiley Online Library or from the author.

Acknowledgements

This material was based upon work supported by the NSF under grant no. EFMA-1830870. S.E. was partially supported by a NASA Space Technology Graduate Research Fellowship (80NSSC21K12690). S.Y.K. was supported by an NSF CAREER award (CMMI-1812948). L.S.-B. was supported by an NSF Human-Centered Computing award (IIS-1954591). T.B. and O.D.Y. were supported by a NASA Early Career Faculty award (80NSSC17K0553). The authors thank Prof. Minjiang Zhong and Prof. Eric Brown for access to testing equipment. The authors thank Dr. Amir Mohammadi Nasab for assistance in editing the manuscript.

Conflict of Interest

The authors declare no conflict of interest.

Author Contributions

S.Y.K. and S.E. contributed equally to this work. S.Y.K. and R.K.-B. conceived the idea. S.Y.K. and S.E. performed the materials design and manufacturing. S.Y.K., S.E., L.S.-B., and T.B. performed the material characterization. S.Y.K., S.E., L.S.-B., and O.D.Y. performed the demonstrations. O.D.Y. performed the additive manufacturing. All authors participated in writing the manuscript.

Data Availability Statement

The data that support the findings of this study are available from the corresponding author upon reasonable request.

Keywords

double emulsion, granular actuators, multicore microcapsules, multiphase composites, phase-change actuators, printable soft actuators, soft robotics

Received: November 25, 2021
Revised: February 5, 2022
Published online: March 10, 2022

[1] F. Schmitt, O. Piccin, L. Barbé, B. Bayle, *Front. Rob. AI* **2018**, *5*, 84.
[2] F. Iida, C. Laschi, *Procedia Comput. Sci.* **2011**, *7*, 99.
[3] D. S. Shah, M. C. Yuen, L. G. Tilton, E. J. Yang, R. Kramer-Bottiglio, *IEEE Rob. Autom. Lett.* **2019**, *4*, 2204.

[4] R. L. Baines, J. W. Booth, F. E. Fish, R. Kramer-Bottiglio, in *2019 2nd IEEE Int. Conf. on Soft Robotics (RoboSoft)*, IEEE, Piscataway, NJ, USA **2019**, pp. 704–710.
[5] R. Baines, S. Freeman, F. Fish, R. Kramer-Bottiglio, *Bioinspiration Biomimetics* **2020**, *15*, 025002.
[6] R. V. Martinez, A. C. Glavan, C. Keplinger, A. I. Oyetibo, G. M. Whitesides, *Adv. Funct. Mater.* **2014**, *24*, 3003.
[7] M. T. Tolley, R. F. Shepherd, B. Mosadegh, K. C. Galloway, M. Wehner, M. Karpelson, R. J. Wood, G. M. Whitesides, *Soft Rob.* **2014**, *1*, 213.
[8] Y. Wu, J. K. Yim, J. Liang, Z. Shao, M. Qi, J. Zhong, Z. Luo, X. Yan, M. Zhang, X. Wang, R. S. Fearing, R. J. Full, L. Lin, *Sci. Rob.* **2019**, *4*, eaax1594.
[9] Y. Mengüç, Y.-L. Park, H. Pei, D. Vogt, P. M. Aubin, E. Winchell, L. Fluke, L. Stirling, R. J. Wood, C. J. Walsh, *Int. J. Rob. Res.* **2014**, *33*, 1748.
[10] R. K. Kramer, C. Majidi, R. J. Wood, in *2011 IEEE Int. Conf. on Robotics and Automation*, IEEE, Piscataway, NJ, USA **2011**, pp. 1103–1107.
[11] Y.-L. Park, B. Chen, N. O. Pérez-Arancibia, D. Young, L. Stirling, R. J. Wood, E. C. Goldfield, R. Nagpal, *Bioinspir. Biomim.* **2014**, *9*, 016007.
[12] A. T. Asbeck, S. M. M. D. Rossi, I. Galiana, Y. Ding, C. J. Walsh, *IEEE Rob. Autom. Mag.* **2014**, *21*, 22.
[13] J. Kwon, J. H. Park, S. Ku, Y. H. Jeong, N. J. Paik, Y. L. Park, *IEEE Rob. Autom. Lett.* **2019**, *4*, 2547.
[14] P. Polygerinos, Z. Wang, K. C. Galloway, R. J. Wood, C. J. Walsh, *Rob. Auton. Syst.* **2015**, *73*, 135.
[15] F. Ilievski, A. D. Mazzeo, R. F. Shepherd, X. Chen, G. M. Whitesides, *Angew. Chem., Int. Ed.* **2011**, *50*, 1890.
[16] E. Brown, N. Rodenberg, J. Amend, A. Mozeika, E. Steltz, M. R. Zakin, H. Lipson, H. M. Jaeger, *Proc. Natl. Acad. Sci. USA* **2010**, *107*, 18809.
[17] A. M. Nasab, A. Sabzehzar, M. Tatari, C. Majidi, W. Shan, *Soft Rob.* **2017**, *4*, 411.
[18] H. Abidi, M. Cianchetti, *Front. Rob. AI* **2017**, *4*, 5.
[19] D. Rus, M. T. Tolley, *Nature* **2015**, *521*, 467.
[20] P. Boyraz, G. Runge, A. Raatz, *Actuators* **2018**, *7*, 48.
[21] C. Majidi, *Adv. Mater. Technol.* **2019**, *4*, 1800477.
[22] N. El-Atab, R. B. Mishra, F. Al-Modaf, L. Joharji, A. A. Alsharif, H. Alamoudi, M. Diaz, N. Qaiser, M. M. Hussain, *Adv. Intell. Syst.* **2020**, *2*, 2000128.
[23] G. K. Klute, J. M. Czerniecki, B. Hannaford, in *1999 IEEE/ASME Int. Conf. on Advanced Intelligent Mechatronics (Cat. No.99TH8399)*, IEEE, Piscataway, NJ, USA **1999**, pp. 221–226.
[24] P. Polygerinos, N. Correll, S. A. Morin, B. Mosadegh, C. D. Onal, K. Petersen, M. Cianchetti, M. T. Tolley, R. F. Shepherd, *Adv. Eng. Mater.* **2017**, *19*, 1700016.
[25] M. Li, X. Wang, B. Dong, M. Sitti, *Nat. Commun.* **2020**, *11*, 3988.
[26] E.-K. Fleischmann, F. R. Forst, K. Köder, N. Kapernaum, R. Zentel, *J. Mater. Chem. C* **2013**, *1*, 5885.
[27] T. Hessberger, L. Braun, R. Zentel, *Polymers* **2016**, *8*, 410.
[28] M. A. Zainal, M. S. M. Ali, in *2016 IEEE EMBS Conf. on Biomedical Engineering and Sciences (IECBES)*, IEEE, Piscataway, NJ, USA **2016**, pp. 76–79.
[29] A. Miriyev, K. Stack, H. Lipson, *Nat. Commun.* **2017**, *8*, 596.
[30] A. Miriyev, G. Caires, H. Lipson, *Mater. Des.* **2018**, *145*, 232.
[31] A. Miriyev, B. Xia, J. C. Joseph, H. Lipson, *3D Print. Addit. Manuf.* **2019**, *6*, 309.
[32] F. Meder, G. A. Naselli, A. Sadeghi, B. Mazzolai, *Adv. Mater.* **2019**, *31*, 1905671.
[33] R. Amirifar, K. Dong, Q. Zeng, X. An, *Soft Matter* **2019**, *15*, 5933.
[34] R. Amirifar, K. Dong, Q. Zeng, X. An, *Soft Matter* **2018**, *14*, 9856.
[35] M. V. Sapozhnikov, Y. V. Tolmachev, I. S. Aranson, W.-K. Kwok, *Phys. Rev. Lett.* **2003**, *90*, 114301.
[36] M. Z. Miskin, H. M. Jaeger, *Nat. Mater.* **2013**, *12*, 326.
[37] S. Nezamabadi, T. H. Nguyen, J.-Y. Delenne, F. Radjai, *Granular Matter* **2016**, *19*, 8.
[38] A. Hemmerle, M. Schröter, L. Goehring, *Sci. Rep.* **2016**, *6*, 35650.
[39] V. Magnanimo, L. La Ragione, J. Jenkins, P. Wang, H. Makse, *Europhys. Lett.* **2008**, *81*, 34006.
[40] R. P. Behringer, B. Chakraborty, *Rep. Prog. Phys.* **2018**, *82*, 012601.
[41] D. Bi, J. Zhang, B. Chakraborty, R. P. Behringer, *Nature* **2011**, *480*, 355.
[42] E. I. Corwin, H. M. Jaeger, S. R. Nagel, *Nature* **2005**, *435*, 1075.
[43] T. S. Majmudar, M. Sperl, S. Luding, R. P. Behringer, *Phys. Rev. Lett.* **2007**, *98*, 058001.
[44] A. J. Liu, S. R. Nagel, *Soft Matter* **2010**, *6*, 2869.
[45] H. T. Chou, S. H. Chou, S. S. Hsiau, *Powder Technol.* **2014**, *252*, 42.
[46] A. K. Grosskopf, R. L. Truby, H. Kim, A. Perazzo, J. A. Lewis, H. A. Stone, *ACS Appl. Mater. Interfaces* **2018**, *10*, 23353.
[47] S. H. Chou, S. S. Hsiau, *Powder Technol.* **2012**, *226*, 99.
[48] T. Ma, R. Yang, Z. Zheng, Y. Song, *J. Rheol.* **2017**, *61*, 205.
[49] A. Jiang, T. Ranzani, G. Gerboni, L. Lekstutyte, K. Althoefer, P. Dasgupta, T. Nanayakkara, *Soft Rob.* **2014**, *1*, 192.
[50] Y. Jiang, D. Chen, C. Liu, J. Li, *Soft Rob.* **2019**, *6*, 118.
[51] E. Steltz, A. Mozeika, J. Rembisz, N. Corson, H. M. Jaeger, in *Electroactive Polymer Actuators and Devices (EAPAD) 2010*, SPIE, Bellingham, WA, USA **2010**, pp. 640–648.
[52] S. G. Fitzgerald, G. W. Delaney, D. Howard, *Actuators* **2020**, *9*, 104.
[53] P. S. Wellborn, N. P. Dillon, P. T. Russell, R. J. Webster, *Int. J. Comput. Assisted Radiol. Surg.* **2017**, *12*, 1069.
[54] A. Cavallo, M. Brancadoro, S. Tognarelli, A. Menciassi, *Soft Rob.* **2019**, *6*, 161.
[55] T. Ranzani, M. Cianchetti, G. Gerboni, I. De Falco, A. Menciassi, *IEEE Trans. Rob.* **2016**, *32*, 187.
[56] J. D. Brigido-González, S. G. Burrow, B. K. Woods, *J. Intell. Mater. Syst. Struct.* **2019**, *30*, 2581.
[57] K. Dierichs, A. Menges, *Granular Matter* **2016**, *18*, 25.
[58] S. Y. Kim, S. Liu, S. Sohn, J. Jacobs, M. D. Shattuck, C. S. O'Hern, J. Schroers, M. Loewenberg, R. Kramer-Bottiglio, *Nat. Commun.* **2021**, *12*, 3768.
[59] M. Loewenberg, E. J. Hinch, *J. Fluid Mech.* **1997**, *338*, 299.
[60] K. M. B. Jansen, W. G. M. Agterof, J. Mellema, *J. Rheol.* **2000**, *45*, 227.
[61] A. Needleman, *Int. J. Solids Struct.* **1977**, *13*, 409.
[62] C. Keplinger, T. Li, R. Baumgartner, Z. Suo, S. Bauer, *Soft Matter* **2011**, *8*, 285.
[63] J. Vaicekauskaite, P. Mazurek, S. Vudayagiri, A. L. Skov, *J. Mater. Chem. C* **2020**, *8*, 1273.
[64] J. W. Boley, S.-H. Hyun, E. L. White, D. H. Thompson, R. K. Kramer, *ACS Appl. Mater. Interfaces* **2016**, *8*, 34171.
[65] T. A. H. Nguyen, M. A. Hampton, A. V. Nguyen, *J. Phys. Chem. C* **2013**, *117*, 4707.
[66] V. Chhasatia, *Ph.D. Thesis*, Drexel University, Philadelphia, PA, USA **2012**.
[67] T. L. Buckner, R. A. Bilodeau, S. Y. Kim, R. Kramer-Bottiglio, *Proc. Natl. Acad. Sci. USA* **2020**, *117*, 25360.
[68] T. J. Ober, D. Foresti, J. A. Lewis, *Proc. Natl. Acad. Sci. USA* **2015**, *112*, 12293.
[69] O. D. Yirmibesoglu, J. Morrow, S. Walker, W. Gosrich, R. Cañizares, H. Kim, U. Daalkhaijav, C. Fleming, C. Branyan, Y. Menguc, in *2018 IEEE Int. Conf. on Soft Robotics (RoboSoft)*, IEEE, Piscataway, NJ, USA **2018**, pp. 295–302.
[70] O. D. Yirmibesoglu, L. E. Simonsen, R. Manson, J. Davidson, K. Healy, Y. Menguc, T. Wallin, *Commun. Mater.* **2021**, *2*, 82.